Bidirectional Coupling of Macroscopic and Microscopic Pedestrian Evacuation Models[1]

André Borrmann[1], Angelika Kneidl[1], Gerta Köster[3,2], Stefan Ruzika[2], and Markus Thiemann[2]

{borrmann, kneidl}@bv.tum.de
[1]Technische Universität München, Arcisstraße 21, 80290 München, Germany

{ruzika, thiemann }@mathematik.uni-kl.de
[2]Technische Universität Kaiserslautern, Paul-Ehrlich-Straße 14, 67663 Kaiserslautern, Germany

gerta.koester@siemens.com
[3]Siemens AG, Corporate Technology, Production Processes, CT PP2, D-80200, Munich, Germany

Corresponding author: kneidl@bv.tum.de, Tel: +49-89-28923062, Fax: +49-89-28925051

Abstract In this contribution, a combination of a macroscopic and a microscopic model of pedestrian dynamics using a bidirectional coupling technique is presented which allows to obtain better predictions for evacuation times. While the macroscopic model is derived from dynamic network flow theory, the microscopic model is based on a cellular automaton. Output from each model is fed into the other, thus establishing a control cycle. As a result, the gap between the evacuation times computed by both models is narrowed down: The coupled model considers both optimized routing strategies as well as microscopic effects. Accordingly the typical underestimation of evacuation times by purely macroscopic approaches is reduced. At the same time the microscopic model is enhanced by a steering component which reflects the macroscopic knowledge and the impact of supervising personnel on the distribution of pedestrian flows.

Keywords: Cellular Automaton, Dynamic Network Flows, Bidirectional Coupling, Control Cycle, Pedestrian Dynamics, Evacuation Modeling

---

1 This research is partly supported by the Federal Ministry for Education and Research (Bundesministerium für Bildung und Forschung, BMBF), Project REPKA, under FKZ 13N9961 (TU Kaiserslautern), 13N9964 (Siemens)

2 Present Address: Hochschule München, Munich University of Applied Sciences, Munich, Lothstr. 34, D-80335 Munich

1 Introduction

Modeling pedestrian dynamics to predict pedestrian behavior for both standard and panic situations has been examined using various approaches as described in [Schadschneider et al. 2009]. One possibility to categorize the different approaches is to distinguish between macroscopic and microscopic models. Macroscopic models focus on overall situations and assume mean values (e.g. densities, velocities). They are widely used for determining minimum evacuation times. Lattice-gas models [Jiang and Wu 2007], fluid-dynamics models [Henderson 1974] and network flow models [Hamacher and Tjandra 2002] fall into this category.

Microscopic approaches on the other hand focus on the behavior of individuals, i.e. they model the movements of individual persons and the interactions between them. These models are able to reproduce microscopic effects observable in reality, such as density-velocity relations, bottlenecks etc. Examples for such models are ASERI [IST 2004], buildingEXODUS [Galea and Galparsoro 1993], F.A.S.T-Model [Kretz and Schreckenberg 2006], PedGo [TraffGo], Simulex [Thompson and Marchant 1994]).

One major objective of modeling pedestrian crowds is to find lower bounds for the evacuation time of a given scenario, including the evacuation of buildings, regions, etc. Network flow-based approaches are capable of providing this information [Chalmet et al. 1982]. They find optimal solutions assuming that each of the involved pedestrians takes routing decisions which result in optimal use of the escape way network and thus in a minimal overall evacuation time. Here, microscopic aspects of pedestrian behavior like interaction are not taken into account. Thus, the determined egress times will in most cases underestimate reality. Nevertheless they can serve as a valid lower bound for evacuation times.

On the other hand, microscopic models take into account interaction and local phenomena such as lane formation, bottlenecks and the slow-down of dense crowds. However, the evacuation times determined by these models cannot serve as a lower bound, as the simulated pedestrians have no overall-knowledge and move according to locally optimal decisions.

To improve the quality of the computed lower bound for evacuation times, we propose to combine both approaches. In the first step, a macroscopic (optimization) model is used which is based on quickest flows in dynamic networks to compute optimal routing strategies [Hamacher and Tjandra 2001]. Then, a microscopic (simulation) model is applied to capture pedestrian behavior and derive a heuristic upper bound. The model is based on a cellular automaton [Burstedde et al. 2001, Emmerich and Rank 1997, Kinkeldey 2003, Klüpfel 2003, Kretz 2007] using a potential field to describe forces acting on individual pedestrians (according to [Schadschneider et al 2009]).

The estimates computed by each of these approaches enclose the true minimum evacuation time like a sandwich [Heller et al. 2010]. In this paper, it is shown how these two approaches can be coupled by means of an iterative control cycle feeding output from one model into the other and vice versa. We get distribution

ratios at each node of the network from the macroscopic model, which guide the pedestrians of the simulation to their target. The simulation on the other hand produces average travel times for each arc while taking into account pedestrian deceleration according to the densities on the arcs. We show that the proposed coupling significantly diminishes the gap between the predicted evacuation times from simulation and optimization.
Few attempts have been made to combine macroscopic and microscopic models for pedestrian dynamics. [Peng 2006] proposed a hybrid model including data of a quickest dynamic network flow in a simulation model. [Dressler et al. 2009] compute an earliest arrival flow in a dynamic network model to assign optimal exits to evacuees in the simulation. In this paper, we go one step further by implementing a full control cycle which does not only improve the results of each individual approach but provides a better estimate of an evacuation time by reducing the gap between microscopic predictions and macroscopic lower bounds.

This article is organized as follows: First, the macroscopic and microscopic models are presented. Then, we specify the setup of the bidirectional coupling relating to the two models. The results and the discussion as well as an outlook on further research conclude the article.

2 Description and Setup of the Macroscopic Model

The scenario (building, region, etc.) is modeled using a discrete-time dynamic network $G = (N, A, T)$, where N is a set of nodes, A is a set of directed arcs, and T is a finite time horizon discretized into the set $\{0,...,T\}$. The node set N subsumes a *source* $s \in N$ and a *target* $t \in N$. Each arc $(i,j) \in A$ has an associated time-dependent *capacity* $u_{ij}(\theta) \in \mathbb{Z}_0^+$ and a time-dependent *travel time* $\tau_{ij}(\theta) \in \mathbb{Z}_0^+$ for all time steps $\theta = 0, ..., T$. Here, $u_{ij}(\theta)$ limits the number of flow units that can enter arc (i,j) at time θ. We assume that the node *capacity* is zero for all nodes and all time steps, i.e. no waiting at nodes is permitted. The travel time $\tau_{ij}(\theta)$ defines the time needed to traverse arc (i,j) for flow departing from node i at time θ, i.e. the flow will arrive at node j at time $\theta+\tau_{ij}(\theta)$.
A *flow* is a function $x : A \times \{0,...,T\} \to \mathbb{Z}_0^+$ which assigns a non-negative value to each arc for all time steps and which is subject to flow conservation (equation (1)) and *capacity* constraints (equation (3)). No flow is left in the network after time T (equation (2)). For a more detailed introduction on network flows we refer readers to the book of Ahuja et al. [Ahuja et al. 1993].

$$\sum_{(j,i)\in A}\ \sum_{\{\theta':\theta'+\tau_{ji}(\theta')=\theta\}} x_{ji}(\theta') -$$

$$\sum_{\{(i,j):(i,j)\in A,\theta+\tau_{ij}(\theta)\le T\}} x_{ij}(\theta) = 0, i \in N \setminus \{s,t\}, \theta = 0,...,T \quad (1)$$

$$x_{ij}(\theta) = 0,\ \theta + \tau_{ij}(\theta) > T, (i,j) \in A \quad (2)$$

$$0 \le x_{ij}(\theta) \le u_{ij}(\theta),\ \theta + \tau_{ij}(\theta) \le T, (i,j) \in A \quad (3)$$

The goal of the *quickest flow problem* (see [Burkard et al. 1993]) is to find a feasible dynamic flow x which sends a given number of flow units $U \in \mathbb{Z}_0^+$ from s to t in the shortest time $T_U \le T$. With the setting given above, the problem is called *discrete-time quickest flow problem with time-dependent attributes.* We refer to [Tjandra 2003] for mathematical details. Tjandra proposed an algorithm to solve this problem by successively finding earliest arrival augmenting paths from source to target in the network. When the total amount of flow augmented along these paths exceeds the initial flow, the time of the last augmenting path determines the quickest flow. In context of evacuation problems, for a given scenario, the value of the quickest flow is the fastest evacuation time for a known number of evacuees from source s to target t. The function x provides a pattern for the optimal evacuation routes in the network.

2.1 Network Setup for Realizing the Coupling

To model pedestrian movements using dynamic network flows, we represent corridors, walkways, and streets etc. in a given scenario as arcs in the network. Every arc $(i,j) \in A$ has a corresponding fixed *width* $w_{ij}[m]$ and *length* $l_{ij}[m]$. In the coupling setup, the maximum possible rate of flow per unit width $M_{ij}[1/ms]$ for every arc $(i,j) \in A$ is predefined, henceforth called the *specific flow rate* (SFR) of arc (i,j). We fix the length of the basic time unit for the network parameters as $z = 1s$. Based on this data we compute the *capacity* as $u_{ij} = \lfloor M_{ij} \cdot w_{ij} \cdot 1/z \rfloor$. Note that the *capacity* is constant over time. Moreover, an *average velocity* $v_{ij}(\theta)$ for every arc $(i,j) \in A$ and $\theta = \{0,...,T\}$ with corresponding *travel time* $\tau_{ij}(\theta) = \lfloor l_{ij} \cdot v_{ij}(\theta) \cdot z \rfloor$ is assumed to be known. Figure 1 shows an example for the network modeling.

Figure 1 Example for modeling a corridor (left) as an arc in the network (right). Assumed velocity v=1.3 m/s, source flow rate M=1.5 (ms)$^{-1}$

3 Description and Setup of the Microscopic Model

The employed microscopic model is based on a cellular automaton [Burstedde et al. 2001, Emmerich and Rank 1997, Kinkeldey 2003, Klüpfel 2003, Kretz 2007]. The whole area of interest is discretized by hexagonal cells, each of which can accommodate an average European male [Weidmann 1992]. At each time step, each cell can be occupied either by a pedestrian, an obstacle, a source or a target. Pedestrians move according to specific behavior rules from sources to targets. The movement of a pedestrian is influenced by different forces, namely the repellent forces of both obstacles and other pedestrians as well as the attraction force of the target. All forces are superimposed and represented by a common potential field. At each time step, each person moves to an accessible neighboring cell with minimum potential field value. Once the target has been reached, the person is removed from the model.

Each pedestrian is created with a certain desired walking speed – the so-called free flow velocity [Schadschneider et al. 2009, Weidmann 1992]. This free flow velocity differs for each pedestrian. Following [Weidmann 1992] a Gaussian distribution of the free flow velocities is assumed. Since time and space are discretized in our approach, the velocities are also discrete. We call each discrete velocity a *velocity class*. The number of velocity classes corresponds to the number of micro time steps subsumed by one macro time step. During one macro time step, each pedestrian can move from one cell to the next as often as his velocity class permits. At the end of each macro time step, the velocities of all pedestrians are synchronized.

Pedestrians are forced to slow down depending on the local density, i.e. the number of pedestrians being present in the surrounding cells. The simulation program has been calibrated to reproduce Weidmann's fundamental diagram [Weidmann 1992]. For a more detailed description of the microscopic model, please refer to [Klein et al. 2010].

3.1 Extensions of the Model for Realizing the Coupling

To implement the coupling approach, we define a graph on top of the cellular automaton that is automatically derived from the underlying topography (Höcker et al. 2010, Kneidl et al. 2011). This is done by creating orientation points on the bisector of each convex obstacle corner. These orientation points refer to graph nodes and each point is subsequently connected to all orientation points in sight by means of an arc. In addition, they are connected to the source and the target in the same manner (see Figure 2). A similar approach for deriving this graph is described in [Chooramun et al. 2010].

This graph, including the arc parameters width and length, is used for the macroscopic setup to construct the network. In the microscopic model, this graph is used to guide the pedestrians to their target, thus replacing the original functionality of both the target and the obstacle function of the potential field. The

target function is now used only for the navigation between two adjacent nodes. The Euclidean distance between these nodes is used as arc weight in the network. The obstacle function is obsolete as intermediate targets are in sight if an arc connects them. The complete setup of the microscopic model is shown in Figure 3.

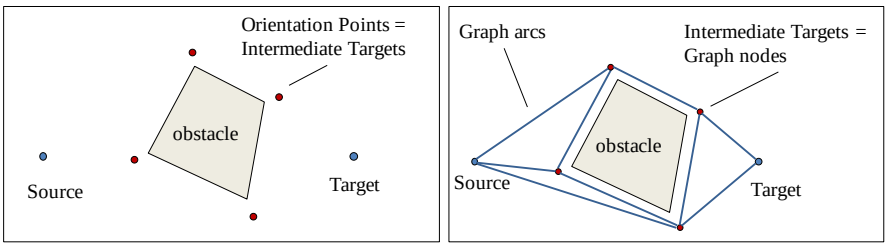

Figure 2 Graph derivation from scenario

In the simulation, a pedestrian traverses along arcs of the graph leading to his target and passing intermediate targets along the way. The macroscopic model yields a distribution ratio for each node, according to which the pedestrians choose their next intermediate target.

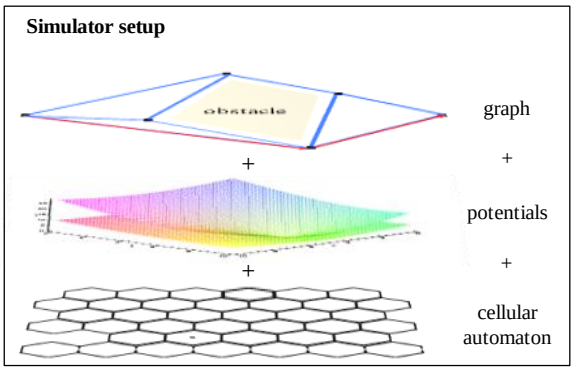

Figure 3 The microscopic model includes three different layers: The cellular automaton, the potential fields and the navigation graph

4 Control Cycle Setup and Constraints for Realizing the Coupling

In this section, the coupling setup is described in detail. First, we describe all parameters which have to be specified for the coupling, followed by a detailed description of the coupling procedure.

4.1 Parameter Description

We define shared (fixed) parameters, summarized in Table 1 and variable parameters, summarized in Table 2. While the former are kept constant during the entire experiment, the latter are adapted in each control cycle. A cycle consists of one optimization run followed by one simulation run.

Name	Description
Scenario	Scenario including network derived with arc width and length
N	Number of pedestrians
t	Time step size
SFR	**S**pecific **f**low **r**ate for all arcs

Table 1 Shared (fixed) parameters

Scenario including the network - A scenario consists of one source and one final target plus some intermediate targets as well as the derived network.

Number of pedestrians - The number of pedestrians has to be large enough to observe interaction between the pedestrians and hence between the two models.

Time step size - The time step size describes the common interval size of the parameter exchange between the two models. In each time step the values of the variable parameters are averaged and adapted by both models, respectively.

Name	Description
DR	**D**istribution **r**atios for each arc and each time step
SFQ	**S**ource **f**low **q**uantity for each time step
v	Average velocity on each arc for each time step

Table 2 Variable parameters

Specific flow rate (*SFR*) for each arc - The *SFR* on an arc corresponds to the maximum number of pedestrians who can move through a unit width in one second along that arc. The *SFR* for each arc is determined within the simulation in a pre-processing phase.

Time-dependent distribution ratios (*DR*) for each arc – DRs refer to flow distributions on all arcs incident to some node, i.e. how is the flow passed from one node to all incident arcs. The ratios sum up to 1 for each node and can differ from time step to time step, thus are time-dependent. DRs are determined by the optimization and are calculated as an average value at each time step. The pedestrians are distributed according to these ratios at the corresponding intermediate targets during the simulation.

Source flow quantity (*SFQ*) for each time step - The source flow quantity refers to the number of flow units leaving the source at each time step in the optimization network. It is generated by the optimization network and used as input for the simulation run: For each time step, the amount of flow leaving the source in the network defines the number of pedestrians to be generated in the corresponding time step of the simulation run. Interaction between pedestrians may prevent the creation of all required pedestrians in a single time step. In this case, they are generated in the subsequent time step.
The number of effectively generated pedestrians is fed back to the optimization to serve as a reference. The adaptation of the flow quantity within the optimization works as follows: if the optimal flow quantity is not achieved in the simulation in a single time step, then the overall capacity of the source (i.e. the total amount of flow that can be sent from the source) in this time step is reduced to the smaller value from the simulation.

Average velocity on each arc for each time step - The simulation returns the average velocities for each arc and time step.
In coupling cycle $i \in \{1,\ldots,number\ of\ coupling\ cycles\}$, these velocities are read in by the optimization in the following manner:

$$v^{i}_{regulation} = \alpha \cdot v^{i}_{simulation} + (1-\alpha) \cdot v^{i-1}_{regulation}$$

Here, $v^{0}_{regulation}$ is the velocity used in the initial dynamic network of cycle zero. The parameter $\alpha \in [0,1]$ refers to the predefined weight of the new average velocities.

Figure 4 gives an overview of all parameters and the way they are exchanged within one coupling cycle.

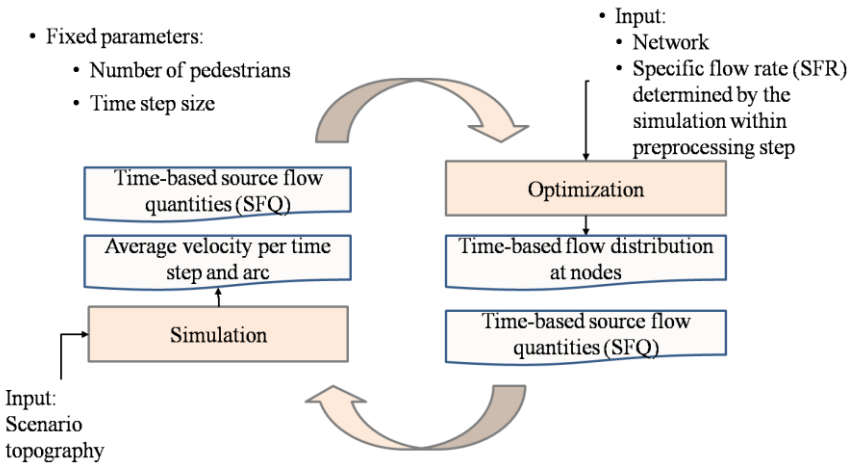

Figure 4 Coupling setup

4.2 The Control Cycle

Before the actual control cycle starts, the specific flow rate (*SFR*) is derived on each arc of the network by means of a pre-processing phase..
The graph which is derived from the scenario within the simulation is extended by the optimization to a dynamic network, establishing it with the static parameters width and length of each arc and adding parameters *capacity* and *travel time* per arc. The capacity of an arc is determined by the given specific flow rate and width whereas the *travel time* is derived from the length of an arc and an assumed walking speed of each pedestrian of 1.34 m/s as suggested in [Weidmann 1992].
The quickest flow is computed in this network with resulting time-dependent flow distribution ratios on each arc and the time-dependent flow quantity of the source. These corresponding values are returned as input parameters for the simulation.
The simulation sends the pedestrians from the source towards the target according to these two variable parameters. We get time-dependent average walking speeds on each arc as a result. The time-dependent travel times of the arcs in the dynamic network are adjusted on the basis of these average velocities. The quickest flow is computed in the modified network, the source quantities and flow distributions are updated and, once again, returned to the simulation. This cycle is repeated for a fixed number of times or until a stopping criterion is satisfied. A stopping criterion can be that the time difference between the Quickest Flow and the egress time derived by the simulation is smaller than a certain threshold, for example.
An example of one cycle is given in Figure 5: Figure 5a shows the preprocessing phase, Figure 5b illustrates the hand-over of the optimization results to the simulation and in Figure 5c the feedback from the simulation back to the optimization is displayed.

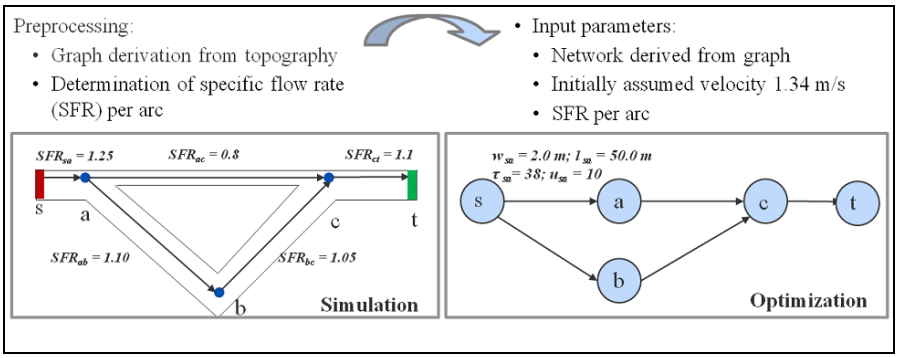

Figure 5a Preprocessing within the simulation derives input parameters for the first optimization run: It derives the graph and determines the SFR, which serves as input for the first optimization run

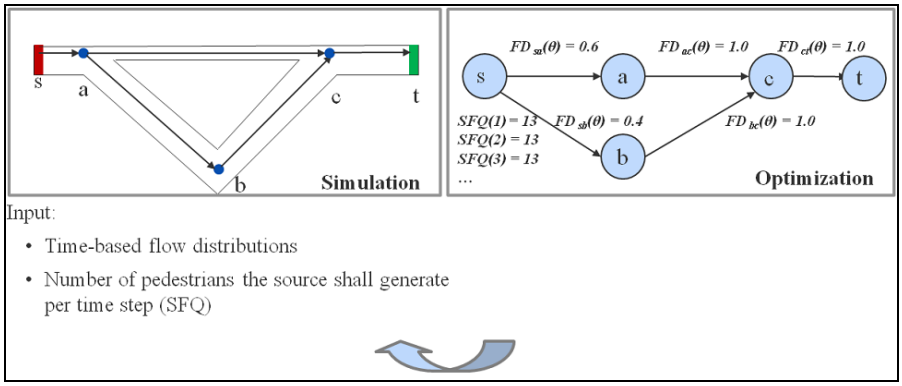

Figure 5b After calculation of quickest flow, the parameters *FD* and *SFQ* for each time step are handed over to the simulation

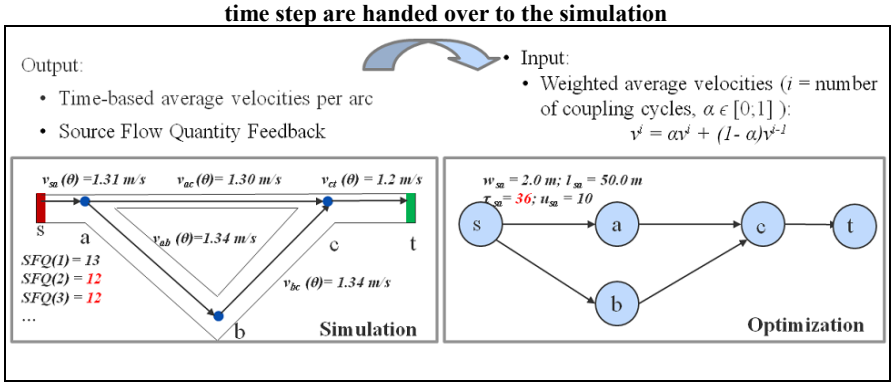

Figure 5c The simulation provides updated velocities and a feedback of the *SFQ* to optimization; the optimization derives updated travel time for each arc; after optimization run, *FD*s and *SFQ*s are updated and handed back to the simulation; the cycle continues as in Figure 5b

5 Case studies

We examined different aspects of the coupling approach: First, we studied the effect of Gaussian-distributed free flow velocities of the pedestrians in the simulation on the coupling and compared it to coupling with uniform free flow velocities of the pedestrians, as we assumed in our previous work [Kneidl et al. 2010].

Secondly, specific scenario setups where the coupling leads to enhancements of both the simulation and optimization were studied. The impact of the coupling with different modifications of a given scenario was inspected. More precisely we examined the benefit of the coupling depending on the capacity of the shortest path through the scenario as well as the influence of n-way intersections within the scenario.

For the simulation, we defined as egress time the moment when 99% of the pedestrians have reached the target. In the simulation, pedestrians may be diverted from their original path onto a secondary path in a dense crowd. Not yet having implemented personal strategy changes, they must resume their original path after it has been cleared. Thus, they may become extreme latecomers. Without applying the 99% rule, they would distort the results. Note, that this rule is applied to overcome a drawback of the simulation, not to ignore stragglers with small free flow velocities. In the following, the egress time is referred to as simulation time. Simulation times are plotted for each cycle starting with the values of "cycle zero" showing the output of both without coupling.

5.1 Choice of fixed parameters

In our previous work [Kneidl et al. 2010] we tested the bidirectional coupling approach on an example scenario with different parameter variations. We showed that the coupling method narrowed the gap between the total evacuation time in the simulation and the time of the quickest flow in the optimization. For certain parameter choices, the improvement became more apparent. In this work, parameter values which have shown to be most suitable for the coupling approach were used. The fixed parameters are shown in Table 3.

Parameter	Value
Number of pedestrians	1,000
α	0.3
Initially assumed velocity (Optimization)	1.34 m/s
Free flow velocity (Simulation)	Gaussian distribution
Number of coupling cycles	25
SFR	Computed in preprocessing phase
Time step size	10 s

Table 3 Parameter overview

We considered three different test cases with this configuration that focus on different aspects to observe effects on our method. The results of our tests are presented in the following.

5.1.1 First Test: Different Free Flow Velocities of Pedestrians in the Simulation

In the real world, the walking behavior of pedestrians varies, e.g. according to age or gender. An individual free flow velocity is assigned to each pedestrian to take this into account. The initially assigned velocity remains unchanged for each individual during all coupling cycles.
We chose a Gaussian velocity distribution following [Weidmann 1992] which is shown in Figure 1.. The coupling is tested with individual velocities on the "triangle example" of Figure 2. For comparison, coupling with a fixed free flow

velocity of 1.34 m/s as proposed in [Kneidl et al. 2010] is carried out. The results are shown in Figure 2.

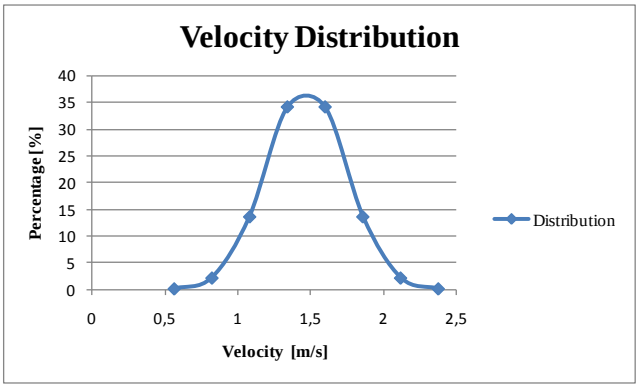

Figure 1 Free-flow velocity distribution according to [Weidmann 1992]

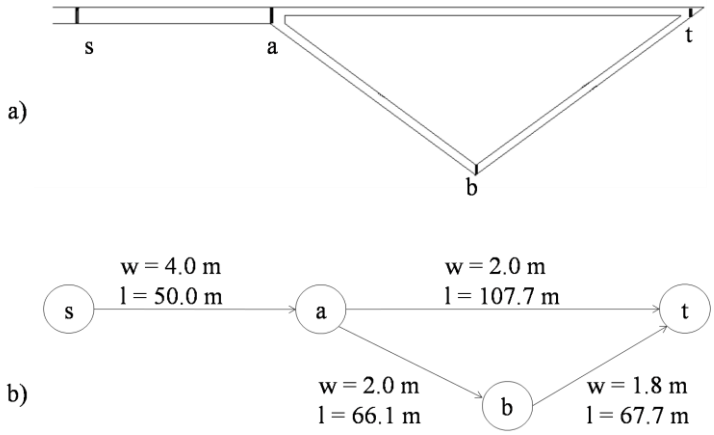

Figure 2 (a) Topography and (b) network of the first test

Figure 3 shows that the gap between the evacuation times of simulation and optimization almost closes for both cases; using uniform free flow velocities and using Gaussian-distributed free flow velocities for the pedestrians.

In the non-coupled simulation ("*cycle zero*"), the evacuation time predicted for Gaussian-distributed free flow velocities is significantly higher than the evacuation time for uniform free flow velocities. With Gaussian-distributed free flow velocities, slow pedestrians occur and will be latecomers, even if they take the shortest path from source to target. Thus, they increase the total evacuation time in the simulation. Therefore we observe higher values of the simulation and optimization times even in the last coupling cycles.

Furthermore, Figure 3 (b) shows that the gap between the evacuation times predicted by simulation and optimization does not close to the same degree in the

setup with Gaussian-distributed free flow velocities as for uniform free flow velocities. This can be explained by a wider variety of initial velocities in the Gaussian-distributed case: For each time step, some of the pedestrians were assigned higher, others a smaller free flow velocity than the average. The travel times on the arcs of the dynamic network are computed by taking the average of all pedestrian velocities on this arc in one time step. Thus, the individual travel time along an arc of pedestrians with small free flow velocities is significantly longer than the average travel time on this arc in the network.

The plot of the simulation time in the case of Gaussian-distributed free flow velocities is not as smooth as in the case of uniform free flow velocities. This is again a consequence of the wider spread of free flow velocities: Since the travel time on each arc in the network is averaged over the individual velocities of the pedestrians on this arc, extreme velocities of individual pedestrians on this arc are not considered. The flow distribution on the arcs, which is handed over to the simulation, is as well an average value for each time step. Altogether, pedestrians with an extreme small or large free flow velocity are either faster or slower than the average; this results in pedestrians reaching nodes at time steps in which they are not expected to do so according to the optimization result. Since this phenomenon cannot be reproduced by the optimization (only average values are used), the simulation cannot reproduce the optimal flow because congestions can occur at intermediate targets.

To sum it up, coupling with different individual velocities still decreases the gap between the egress times of the micro- and macroscopic model like in the case of coupling with uniform free flow velocities. However, the results in the first case are not as smooth as they are in the latter. Nevertheless, individual free flow velocities are more realistic for modeling pedestrian dynamics than uniform free flow velocities; hence the slightly declined results are acceptable.

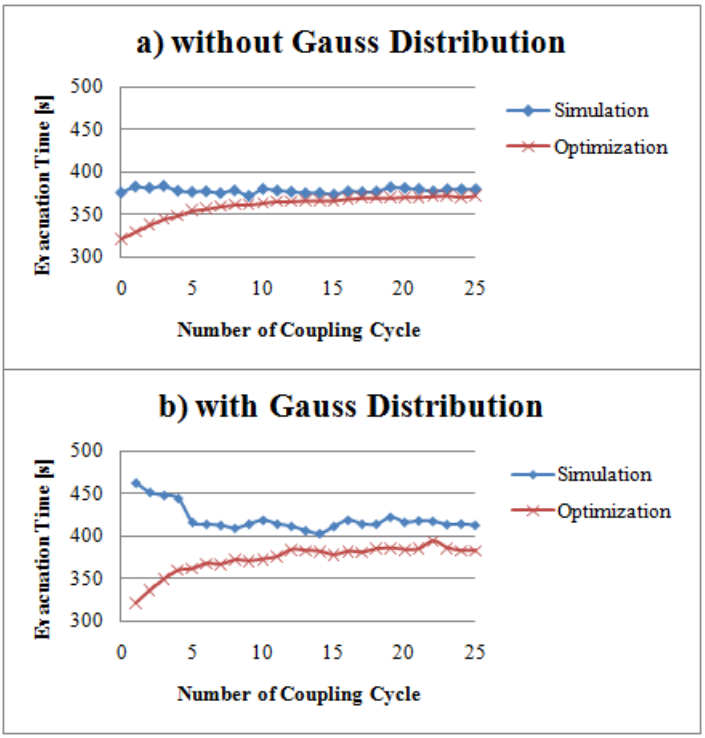

Figure 3 Results of the first test. (a) without Gaussian-distributed free flow velocities (b) with Gaussian distribution of the free flow velocities

5.1.2 Second Test: Variation of the Capacity of the Shortest Path

To determine scenario settings for which the coupling leads to a significant improvement of the microscopic approach, we varied the width of the shortest path of a scenario and examined the effects on the coupling. The test scenario is a simple triangular passageway with an additional corridor. The topography is shown in Figure 2a, the corresponding network can be seen in Figure 4, respectively. The coupling was run with a varying width of the bottleneck of the shortest path, i.e. the corridor between orientation points *a* and *t* is successively chosen as 0.5 m, 1 m, 2 m, and 4 m. The results are summarized in Figure 5.

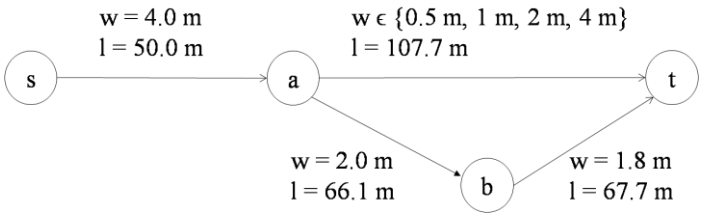

Figure 4 Network of second test

Figure 5 shows, that for each of the four different choices of width, the gap between the evacuation times of simulation and optimization closes during the coupling.

The time corridor of the steady state decreases with the width of the corridor *a-t,* from 460 s to 550 s for $w = 0.5$ m and from 370 s to 400 s for $w = 4$ m. For a wide *a-t*-path, the shortest path from *s* to *t* has a large capacity. Thus, the majority of the pedestrians can take the shortest path without causing congestion and the evacuation time is small. In contrast, a narrow *a-t*-path has a smaller capacity, hence more pedestrians are routed through the longer way from *s* via *a* and *b* to *t*. The overall evacuation time increases.

The evacuation time of the non-coupled simulation is displayed in cycle zero of each plot. In these simulation runs, all pedestrians take the shortest path from *s* via *a* to *t*. We observe that the simulation time significantly increases with decreasing the width of the *a-t*-corridor. The reason for this behavior is on the one hand that for an *a-t*-corridor which is narrower than the corridor from *s* to *a*, congestion in front of the bottleneck *a* occurs. On the other hand, pedestrians with a small free flow velocity slow down their faster followers because overtaking is more difficult in a narrow corridor. In the case of w=0.5 m, overtaking in the *a-t*-corridor is not possible at all, since the cell size in the cellular automaton prevents two cells abreast in the corridor. This effect leads to fluctuations of the simulation time: If in one coupling cycle, a pedestrian with a late starting time has a small free flow velocity and takes the *a-t*-corridor, he will slow down his followers on this corridor and decrease the total evacuation time. In another coupling cycle, this pedestrian takes the wider path from *a* via *b* to *t*. In this case, he can be overtaken by his followers; they will arrive at *t* earlier. Since the simulation time represents the time when 99% of the pedestrians have reached *t*, this one slow pedestrian will not influence the simulation time.

We observe that the non-coupled simulation time is improved by the coupling for the width $w \in \{0.5 \text{ m}, 1 \text{ m}, 2 \text{ m}\}$. The optimization sends some pedestrians along the longer path from *s* via *a* and *b* to *t.* This results in a bigger throughput at *a,* thus the overall evacuation time decreases. The narrower the *a-t*-corridor is, the more significant this effect. For an *a-t*-corridor of 4 m width, the capacity of this corridor is as big as the capacity of the *s-a*-corridor, hence congestion does not occur and the coupling does not improve the simulation time.

Summarized, we identified scenario settings within this experiment for which the coupling leads to an improvement of the simulation time: If the capacity of the shortest path is smaller than the capacity of the arcs defining the longer route to the target, the optimization can help to increase the egress time of the simulation. If the shortest path has a capacity which is the same as the path in front of intersections, the optimization does not contribute any optimal routing as the shortest path is the best path to walk for all pedestrians. For all choices of widths we observed a rise in the optimization times as the effect of pedestrian interaction is taken into account in the network flow model.

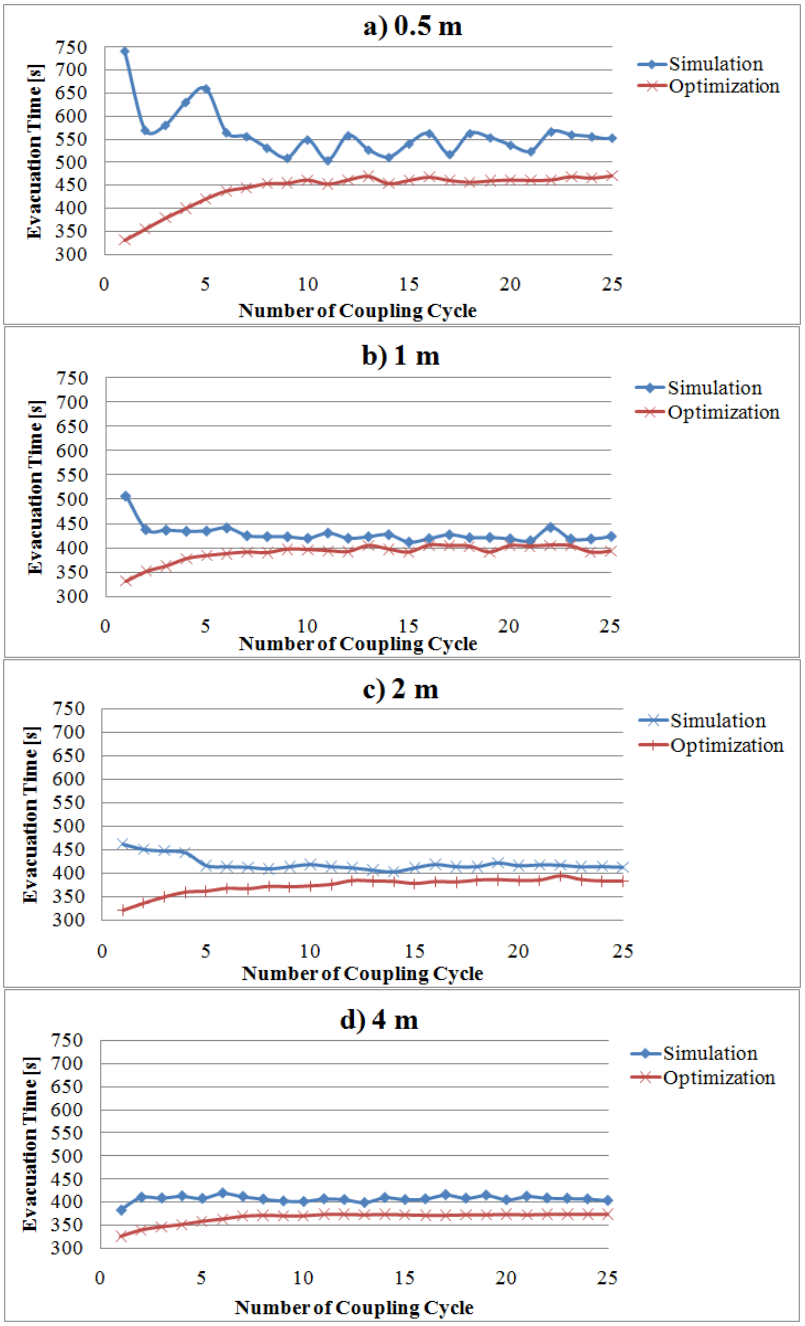

Figure 5 Results of the second test for width of corridor *a-t* (a) 0.5 m, (b) 1 m, (c) 2 m, (d) 4 m

5.1.3 Third Test: Three-way Intersection

As a third aspect we examined the influence of n-way intersections to our method. Therefore, a scenario was constructed, in which the route to the target splits into three possible routes at node *a*. The shortest way has the smallest capacity; both remaining routes are symmetric and are about one and a half times longer. The sum of the width of all three possible routes is the same as the corridor width in front of the intersection. The scenario and the corresponding network are shown in Figure 6.

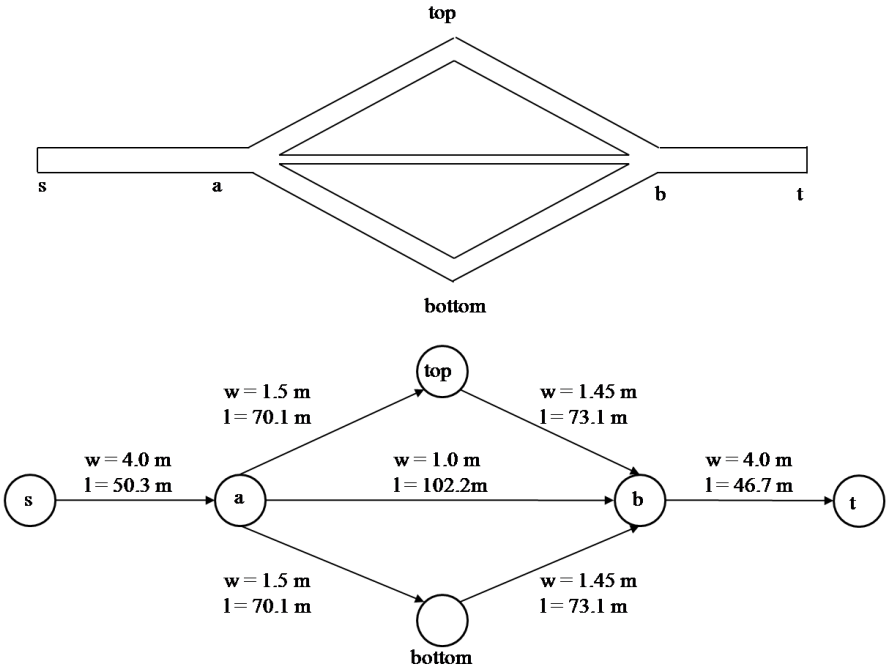

Figure 6 Setup for three-way intersection test

The results of the coupling procedure are shown in Figure 7. The simulation and optimization egress times approximate during the first six coupling cycles and remain close to each other with an average gap of five seconds. The remaining oscillations are explained by the interaction between the pedestrians at the intersection of node *a.* Since some pedestrians at the top of the corridor are assigned the bottom route to continue and vice versa, they interfere with each other and hence produce congestions at the intersection. Nevertheless the result reflects a typical control cycle with small oscillations.

Once again it can be observed that the optimization delivers distribution ratios at the intersection to lower the total egress time of the simulation.

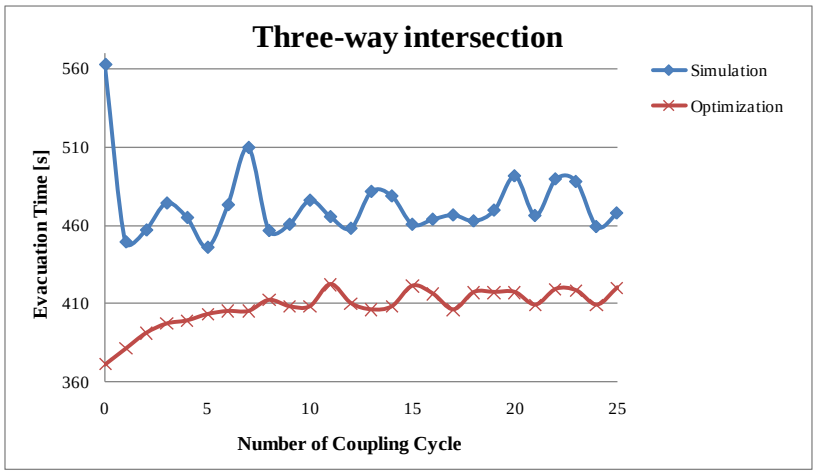

Figure 7 Results of the three-way intersection test

Summarizing all presented tests, we observe that the egress time of the non-coupled simulation ("*cycle zero*") is reduced within the coupling by about 20 to 25 percent by taking into account optimal routing strategies in the simulation. The optimization times of the first coupling cycles increased around 10 to 25 percent compared to later coupling cycles due to updated travel times.
In general we observe that the more influencing route-choices exist in the scenario the more both models are enhanced by the coupling method.
The gap between both models remains (depending on the scenario settings) between 60 seconds (~15 percent of the mean time between both plots) for the "three-way"-example and around 10 seconds (~ 5 percent) for the "shortest way"-example.

6 Conclusion

In this article, a method for combining a microscopic and a macroscopic pedestrian evacuation model in a control cycle has been presented. We studied several test scenarios with uniformly and Gaussian distributed free flow velocities to better capture pedestrian behavior. For both choices of free flow velocities, it was demonstrated that the evacuation times predicted by the simulation as well as the lower bounds derived from optimization, narrow and approach steady states.
Also, the impact of the optimization on the simulation was studied for different scenario settings. The width of the shortest way to the target was varied and the egress time of the simulation was examined: The smaller the capacity of the shortest way the greater the influence of the optimization on the simulation. We observed a clear decrease of the egress times of the simulation with each control cycle.

Our method leads to the following improvements for all tested aspects:
The simulation benefits from the routing which is induced by the results of the optimization. Pedestrians are distributed on the available paths according to the routing determined by optimizing the dynamic network flow. As a result, corridors are less congested and the egress time decreases. This reflects the macroscopic knowledge and the impact of supervising personnel on the distribution of pedestrian flows. The latter is typically realized by placing security staff at specific points such as intersections to route the pedestrians.
Moreover, the optimization model delivers improved lower bounds for the evacuation times. This follows from adjusted travel times on the network arcs, which are refined by the coupling. More precisely, the travel times are adjusted by taking an average of individual, Gaussian distributed velocities. Thus, individual, microscopic aspects are transferred to the macroscopic model, and therefore, the overall egress time of the optimization model reflects Weidmann's measured density-velocity relation of pedestrians.

In the tests presented in this paper we could show, that the gap between the egress times predicted by microscopic simulation and macroscopic optimization narrows down significantly using the coupling approach. It will have to be investigated further under which assumptions a better convergence could be expected. Also, in several cases, we did not manage to completely dampen the oscillations of the simulation from one control cycle to the next. Here a statistically derived averaged velocity may improve the situation.

7 Outlook

The results for simple scenarios that focus on important aspects of pedestrian evacuation presented encourage us to apply our technique on general, more complex evacuation scenarios.
A next step will be to run the coupling procedure on scenarios representing complete buildings or a street scene with more intersections and a more complex overall geometry.
The challenges of generalizing our approach include the following questions:

- How can the derived graph be mapped to rooms inside a building?
- How can the width of a graph arc be defined more generally?
- Do subsequent intersections lead to further oscillations?
- Will the gap between the computed egress times of both models still narrow significantly?

Up to now, we have only modeled scenarios with one source and one target. Evacuation scenarios usually consist of multiple starting points and safety areas. Accordingly, future work will be undertaken in upgrading the coupling approach

so that it can handle scenarios with multiple sources and targets. The presented cellular automaton can be extended to the multiple sources and targets case without additional effort. In a dynamic network model, the quickest flow problem is extended to a multiple sources and targets network flow problem by the *quickest transshipment problem* [Hoppe and Tardos 1995, Miller-Hooks and Stock Patterson 2004].

8 References

Ahuja, R.K., Magnanti, T.L., Orlin, J.B., 1993. Network Flows: Theory, Algorithms, and Applications. Prentice Hall, Englewood Cliffs, New Jersey.

Burkard, R., Dlaska, K., Klinz, B., 1993. The Quickest Flow Problem. ZOR Methods and Models of Operations Research 37, pp. 31-58.

Burstedde, C., Klauck, K., Schadschneider, A., Zittartz, J., 2001. Simulation of Pedestrian Dynamics Using a 2-dimensional Cellular Automaton. Physica A 295, 507-525.

Chalmet, L. G., Francis, R.L., Saunders, P.B., 1982. Network Models for Building Evacuation. Management Science 28, pp. 86-105.

Chooramun, N., Lawrence, P.J., Galea, E.R., 2010. Implementing a Hybrid Space Discretisation Within An Agent Based Evacuation Model. In: R.D. Peacock, E.D. Kuligowski & J.D. Averill (Eds), pp. 449-458, Pedestrian and Evacuation Dynamics, Springer, Berlin Heidelberg.
.

Dressler, D., Groß, M., Kappmeier, J.-P., Kelter, T., Kulbatzki, J., Plümpe, D., Schlechter, G., Schmidt, M., Skutella, M., Temme, S., 2010. On the Use of Network Flow Techniques for Assigning Evacuees to Exit. Procedia Engineering 3, pp. 205-215.

Emmerich, H., Rank, E., 1997. An Improved Cellular Automaton Model for Traffic Flow Simulation. Physica A 234, pp. 676-686.

Galea, E.R., Perez Galparsoro, J. M., 1993. EXODUS: An Evacuation Model for Mass Transport Vehicles. UK CAA Paper 93 006.

Hamacher, H. W., Tjandra, S. A., 2002. Mathematical Modelling of Evacuation Problems: A State of the Art. In: M. Schreckenberg and S.D. Sharma (Eds.), Pedestrian and Evacuation Dynamics, pp. 227-266, Springer, Berlin Heidelberg.

Hamacher, H. W., Heller, S., Klein, W., Köster, G., Ruzika, S., 2010. A Sandwich Approach for Evacuation Time Bounds. In: R.D. Peacock, E.D. Kuligowski & J.D. Averill (Eds), pp. 503-514, Pedestrian and Evacuation Dynamics, Springer, Berlin Heidelberg.

Henderson, L.F., 1974. On the fluid mechanics of human crowd motion. Transportation Research, vol. 8, no. 6, pp. 509–515.

Höcker, M., Berkhahn, V., Kneidl, A., Borrmann, A., Klein, W. , 2010. Graph-based approaches for simulating pedestrian dynamics in building models. Proceedings of the 8th European Conference on Product and Process Modeling

Hoppe, B., Tardos, É., 1995. The Quickest Transhipment Problem. Proceedings of the sixth annual ACM-SIAM symposium on Discrete algorithms, pp. 512-521.

IST: ASERI (Advance Simulation of Evacuation of Real Individuals), 2004. A model to simulate evacuation and egress movement based on individual behavioral response. http://www.ist-net.de/.

Jiang, R. & Wu, Q. , 2007. Pedestrian behaviors in a lattice gas model with large maximum velocity, Physica A: Statistical and Theoretical Physics, vol. 373,683–693.

Kinkeldey, C., 2003. Fussgängersimulation auf der Basis zellulärer Automaten: Studienarbeit im Fach Bauinformatik. Universität Hannover.

Klein, W., Köster, G., Meister, A., 2010. Towards the Calibration of Pedestrian Stream Models. Lecture Notes in Computer Science: PPAM 2009, pp. 521-528, Springer, Berlin Heidelberg.

Klüpfel, H., 2003. A Cellular Automaton Model for Crowd Movement and Egress Simulation. PhD thesis, Universität Duisburg–Essen.

Klüpfel, H., Schreckenberg, M., Meyer-König, T., 2004. Models for Crowd Movement and Egress Simulation. In: Hoogendoorn et al. (Eds.), Traffic and Granular Flow '03, pp. 357-372, Springer, Berlin Heidelberg.

Kneidl, A., Thiemann, M., Borrmann, A., Ruzika, S., Hamacher, H. W., Köster, G., Rank, E., 2010. Bidirectional Coupling of Macroscopic and Microscopic Approaches for Pedestrian Behavior Prediction. In: R.D. Peacock, E.D. Kuligowski & J.D. Averill (Eds), pp. 459-470, Pedestrian and Evacuation Dynamics, Springer, Berlin Heidelberg.

Kneidl, A., Borrmann, A., Hartmann, D., 2011. Generating sparse navigation graphs for microscopic pedestrian simulation models. Proceedings of European Group for Intelligent Computing in Engineering Workshop 2011.

Kretz, T., 2007. Pedestrian Traffic. Simulation and Experiments. PhD thesis, Universität Duisburg-Essen.

Kretz, T., Schreckenberg, M., 2006. The F.A.S.T.-Model. In: El Yacoubi. et al. (Eds.), Cellular Automata - 7th International Conference on CA for Research and Industry, pp. 712–715, Springer, Berlin Heidelberg.

Miller-Hooks, E., Stock Patterson, S., 2004. On Solving Quickest Time Problems in Time-Dependent, Dynamic Networks. Journal of Mathematical Modelling and Algorithms 3, pp. 39-71.

Peng, L., 2006. A Dynamic Network Flow Optimization for Large-Scale Emergency Evacuation. PhD thesis, University of Hong Kong.

Schadschneider, A., Klingsch, W., Kluepfel, H., Kretz, T., Rogsch, C., Seyfried, A., 2009. Evacuation Dynamics: Empirical results, Modeling and Applications. In: R.A. Meyers (Ed.), Encyclopaedia of Complexity and System Science Vol. 3, pp. 3142-3176, Springer, Berlin Heidelberg.

Thompson, P. A., Marchant, E. W., 1994. Simulex; Developing New Computer Modelling Techniques for Evaluation. Fire Safety Science - Proceedings of the 4th International Symposium, pp. 613-624.

Tjandra, S.A., 2003. Dynamic Network Optimization with Application to the Evacuation Problem. PhD thesis, Universität Kaiserslautern, Shaker, Aachen.

TraffGo Handbuch: www.traffgoht.com/de/pedestrians/downloads/index.html

Weidmann U., 1992. Transporttechnik der Fussgänger. Schriftenreihe des IVT 90, Zürich.